LBNL-40097
UC-405
Preprint

ERNEST ORLANDO LAWRENCE
BERKELEY NATIONAL LABORATORY

What is a Natural Norm for Multi Channel Image Processing

Ron Kimmel
Computing Sciences Directorate
Mathematics Department

March 1997
To be submitted
for publication

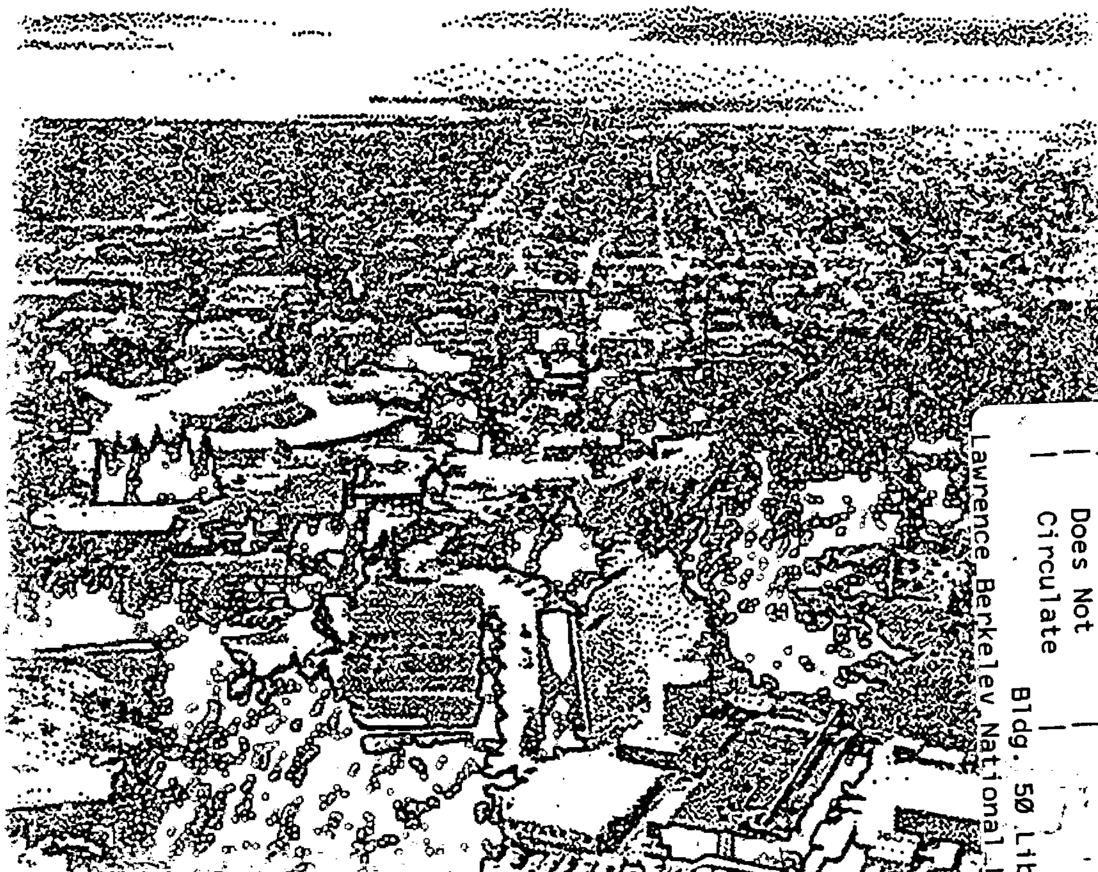

What is a Natural Norm for Multi Channel Image Processing

Ron Kimmel*
Lawrence Berkeley National Laboratory
and Dept. of Mathematics
University of California, Berkeley, CA 94720

Abstract

We show that the geometrical framework, in which color images are considered as surfaces, is meaningful and natural for multi channel image processing. The steepest descent flow associated with the first variation of the area functional is a significant selective smoothing procedure. Generally, the steepest descent flow for multi channel variational methods smoothes the different channels of the image. The functional, or "norm", should capture the way we want the smoothing process to act on the different channels while exploring the coupling between them. Here we justify the usage of the area norm obtained by the geometric framework, and the Belframi steepest descent flow as its natural scale-space, in the multi-channel case. We list the requirements, compare to other recent norms, relate to line element methods in color, and present simulation results.

1 Introduction

Recently, [30, 14, 12, 13], a geometrical framework for image diffusion was introduced. The idea is simple for a gray level image $I(x, y)$ that is considered as the surface $(x, y, I(x, y))$ in the Euclidean space (x, y, I). Yet, it becomes less intuitive for multi channel images. A good example is a color image, which is viewed as a 2D surface $(x, y, R(x, y), G(x, y), B(x, y))$, in the 5D (x, y, R, G, B) space.

It was claimed that a natural norm for image processing is given by minimizing the area of these surfaces in a special way. This norm may serve for intermediate asymptotic analysis in low level vision, that is referred to as 'scale space' in the computer vision community [22]. The norm may be coupled with variance constraints that are implemented via projection methods that were used for convergence based denoising [23] for image processing. Another

*This work is supported in part by the Applied Mathematics Subprogram of the Office of Energy Research under DE-AC03-76SFOOO98, and ONR grant under NOOO14-96-1-0381.

popular option is to combine the norm with lower dimensional measures to create variational segmentation procedures, like the Mumford-Shah [18]. In this note we justify the usage of the area norm obtained by the geometric framework and the Beltrami flow as its natural scale-space. In order to simplify the discussion, we will limit our comparisons to variational methods in non linear scale space image processing, and to Euclidean spaces. See, [21, 36] for non variational methods. That means that the given color space (multi channel space, or feature space) is considered to be Euclidean; the flow is invariant to any Euclidean change of the color coordinates, and is obviously invariant to Euclidean transformations in the spatial domain (translations and rotations of the xy coordinates). Note that given any significant group of transformations in color space, one could design the invariant flow with respect to that group based on the philosophy of images as surfaces: The question then is the meaningful definition of an invariant arclength in the (x, y, R, G, B) hybrid space.

The structure of this note is as follows: Section 2 is a brief overview on the geometric framework for image processing and the Beltrami flow. In Section 3 we list the coupling requirements for the multi channel case. We show that for a simple 'color image formation' model, the natural order of events is captured by the area norm (after scaling different color channels). The relation to line element theory is given. We then present some experimental results of the Beltrami flow in color, and review previous norms. Section 4 summarizes the different norms and justifies the area norm as a natural selection.

2 The Geometric Framework: Brief Overview

A new geometrical framework for image processing was introduced in [30, 14, 12, 13]. This framework finds a seamless link between the TV-L_1 ($\int |\nabla I|$), [23], and the L_2 ($\int |\nabla I|^2$) norms that are often used in image processing, based on the geometry of the image and its interpretation as a surface. It unifies most of the current 'scale space' models for images by a simple selection of one parameter, yet more important, it enables to introduce new methods to deal with images in a simple and natural way.

A functional called "Polyakov action", borrowed from high energy physics, was shown to be useful for image enhancement in color, texture, volumetric medical data, movies, and more. The idea is to consider images as surfaces rather than functions. Then, minimize the area of the surface in a special way; e.g. a gray level image is considered to be a 2D surface given by the graph $I(x, y)$ in the 3D space (x, y, I). Similarly, a color image is a 2D surface that is given by the three graphs: $R(x, y), G(x, y)$, and $B(x, y)$, in the 5D space (x, y, R, G, B).

Consider a gray level image as a map from a two dimensional surface to a three dimensional space ($\mathbb{R}^3$). We have at each point of the xy coordinate plane an intensity $I(x, y)$. The $\mathbb{R}^3$ has Cartesian coordinates (x, y, I) where x and y are the *spatial* coordinates and I is the *feature* coordinate. Now, assume the image is corrupted by an unknown noise and should be 'denoised', or a 'clean' image should be produced for further processing. The idea of geometric selective smoothing [2, 1] is extended to construct a scale space for images in color space, movies, and other multi dimensional images. The idea is to invent a flow that minimizes the area of the image as a surface in a way that preserves the edges.

An important question is how to treat multi channel images. A color image is a good example since one actually considers 3 images Red, Green, and Blue, that are composed into one. To answer this question, we view images as *embedding maps*, that flow towards *minimal surfaces.*

Let us draw a rough sketch of the method: As a first step define an arc-length in the relevant space. For example, an arclength in the (x, y, I) Euclidean space is given by

$$ds^2 = dx^2 + dy^2 + dI^2.$$

Next the *induced metric* of the image surface given by the graph surface $(x, y, I(x, y))$ is 'pulled back' from the arclength equation. By applying the chain rule $dI = I_x dx + I_y dy$, the metric in this case is obtained by rearranging the terms at the arclength definition. The result is the bilinear structure that measures distance on the surface via the arclength

$$ds^2 = g_{11}dx^2 + 2g_{12}dxdy + g_{22}dy^2,$$

where $g_{11} = 1 + I_x^2$, $g_{22} = 1 + I_y^2$, and $g_{12} = I_x I_y$ are the induced metric coefficients. In a similar way, the distance measure and the induced metric, are pulled back from the arclength definition for the 2D surface described by a color image in the 5D (x, y, R, G, B) space. Where now the arclength is given by

$$ds^2 = dx^2 + dy^2 + dR^2 + dG^2 + dB^2.$$

See [38] for a non variational related effort.

The induced metric $g_{\mu\nu}$ is plugged into an action which is the most general form for measuring area. This functional, for two dimensional surface, was first proposed by Polyakov [20] in the context of high energy physics. In the next section we will further elaborate on the selection of area as a proper measure for color images.

Denote by (Σ, g) the image manifold[1] and its metric and by (M, h) the space-feature manifold and its metric[2], then the map $\mathbf{X} : \Sigma \to M$ has the following weight [3]

$$S[X^i, g_{\mu\nu}, h_{ij}] = \int d^m\sigma \sqrt{g} g^{\mu\nu} \partial_\mu X^i \partial_\nu X^j h_{ij}(\mathbf{X}), \qquad (1)$$

where m is the dimension of Σ, g is the determinant of the image metric, $g^{\mu\nu}$ is the inverse of the image metric, the range of indices is $\mu, \nu = 1, \ldots, \dim \Sigma$, and $i, j = 1, \ldots, \dim M$, and h_{ij} is the metric of the embedding space. We used the Einstein summation convention: The

[1]For 2D surfaces $\Sigma = (\sigma_1, \sigma_2)$ is the parametrization, that we later identify with the image plane, i.e. $\sigma_1 = x$, $\sigma_2 = y$. $(g_{\mu\nu})$ here is the metric of the surface, and can be written as a 2×2 matrix:

$$(g_{\mu\nu}) = \begin{pmatrix} g_{11} & g_{12} \\ g_{12} & g_{22} \end{pmatrix}.$$

[2]M for our color case stands for the (x, y, R, G, B) space, and its metric $(h_{\mu\nu})$ is a 5×5 matrix that describes the way we measure distances in this space. We can consider the simple Euclidean color space in which $h_{\mu\nu} = \delta_{\mu\nu}$, i.e. the identity matrix. However, other selections that describe different measures in the color space are possible.

[3]For our color case $\mathbf{X} = (x(\sigma_1, \sigma_2), y(\sigma_1, \sigma_2), R(\sigma_1, \sigma_2), G(\sigma_1, \sigma_2), B(\sigma_1, \sigma_2))$.

summation is applied on each index that appears twice, once as a subscript and once as a superscript. [4]

Given the above functional, we have to choose the minimization. In [30] it was shown how different choices yield different flows. Some flows are recognized as existing methods like the heat flow, with passive coordinate transformation [9], the Perona-Malik flow [19], the minimal surface segmentation [4], the color flow [25, 5], the mean-curvature flow [17] and its variants [7]. The new result in [30, 13] is the steepest descent flow that results by minimizing with respect to the metric itself and the feature coordinates.

The minimization of Polyakov action yields the steepest decent direction for area minimization. If we vary with respect to the metric and the feature coordinate (fixing the x and y coordinates for the gray level and color images), we obtain the area minimization direction given by Beltrami operator operating on the feature coordinate(s). Evolving the image using this result, yields the most efficient geometric flow for smoothing the image while preserving the edges. It is written as

$$\mathbf{I}_t = \Delta_g \mathbf{I}, \tag{2}$$

where for the color case $\mathbf{I} = (R, G, B)$. The operator that is acting on $\mathbf{I}$ is the natural generalization of the Laplacian from flat spaces to manifolds and is called *the second order differential parameter of Beltrami*, or for short *Beltrami operator*, and is denotes by Δ_g. It is defined by

$$\Delta_g \mathbf{I} \equiv \frac{1}{\sqrt{g}} \partial_\mu (\sqrt{g} g^{\mu\nu} \partial_\nu \mathbf{I}). \tag{3}$$

Explicitly, for multi channel $2D$ surfaces, the flow is given by

$$I_t^i = \frac{1}{g}\left(p_x^i + q_y^i\right) - \frac{1}{2g^2}\left(g_x p^i + g_y q^i\right) \tag{4}$$

where $g_x = \partial_x g$ $(g_y = \partial_y g)$, $g_{\mu\nu} = \delta_{\mu\nu} + \sum_i I_\mu^i I_\nu^i$, $g = g_{11}g_{22} - g_{12}^2$, and

$$\begin{aligned} p^i &= g_{22} I_x^i - g_{12} I_y^i, \\ q^i &= -g_{12} I_x^i + g_{11} I_y^i. \end{aligned} \tag{5}$$

Geometrically, for the gray level case, the above evolution equation is the mean curvature flow of the image surface divided by the induced metric $g = \det(g_{\mu\nu})$. Equivalently, it is the evolution via the $\mathbf{I}$ components of the mean curvature vector $\mathbf{H}$. I.e. for the surface $(\mathbf{x}(\sigma_1, \sigma_2), \mathbf{I}(\sigma_1, \sigma_2))$ in the Euclidean space $(\mathbf{x}, \mathbf{I})$, the curvature vector is given by $\mathbf{H} = \Delta_g(\mathbf{x}(\sigma_1, \sigma_2), \mathbf{I}(\sigma_1, \sigma_2))$. If we identify $\mathbf{x}$ with σ then $\Delta_g I^i(\mathbf{x}) = \mathbf{H} \cdot \hat{I}^i$, i.e. the $\hat{I}^i$ component of the mean curvature vector. Observe that this direct computation applies for co-dimensions > 1. The determinant of the induced metric matrix $g = \det(g_{ij}) (= 1 + I_x^2 + I_y^2$ for the gray level case) may be considered as a generalized form of an edge indicator. Therefore, the

[4] Let us consider the simple example of a gray level image $\mathbf{X} = (x(\sigma_1, \sigma_2), y(\sigma_1, \sigma_2), I(\sigma_1, \sigma_2))$. If we identify the x, y plane with the parametrization manifold Σ, and consider a Euclidean space $h_{\mu\nu} = \delta_{\mu\nu}$, we get the area element $\sqrt{g} = \sqrt{1 + I_x^2 + I_y^2}$, and the area measure is then given by $S = \int dxdy \sqrt{1 + I_x^2 + I_y^2}$, or for short we will denote the area norm $\int \sqrt{g}$.

A different, yet very important demand for multi channel image processing is the alignment requirement of the different channels in scale. That is, we want the different channels to align together as they become smoother in scale. Figure 1 shows one level set of each of the three color channels and the corresponding gradient ∇I^i at one point along the level set.

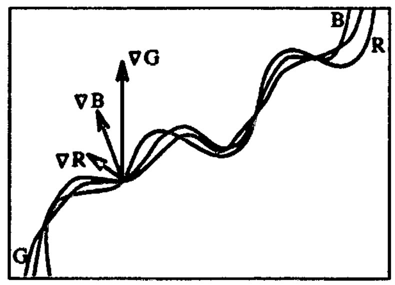

Figure 1: One level set of each of the the channels (R, G, B) are displayed with their corresponding gradient vector at one point.

The requirement that the different channels align together as they evolve, amounts to minimizing the cross products between their gradient vectors $(\nabla I_i, \nabla I_j)^2$, see Figure 2.

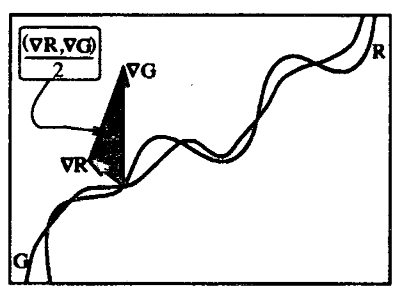

Figure 2: The cross product between the ∇R and ∇G is a measure for the alignment between the two channels: We denote it by $\frac{(\nabla G, \nabla R)}{2}$, which is given by the area of the gray triangle.

On inspection of Eq. (7), the minimization includes the gradient magnitudes of the channels and the cross products between the different channels, which is a desired norm. Next we consider an axiomatic approach for the above claims that will set the order of events and lead us to the area minimization via the Beltrami flow.

3.1 An Axiomatic Approach

Let us define a simple 'image formation' procedure for a color image and extract the order of events for the multi channel processing. One simplified model for color images is a result of viewing Lambertian surface patches. Such a scene is known as a 'Mondrian world'. In this case, each channel may be considered as the projection of the real 3D world surface normal flow (2) is a selective smoothing mechanism that preserves edges and can be generalized to any dimension. For gray level images $\mathbf{I} = I$, the Beltrami flow is given explicitly by

$$I_t = \Delta_g I = \frac{1}{\sqrt{g}}\text{div}\left(\frac{\nabla I}{\sqrt{g}}\right) = \frac{(1+I_x^2)I_{yy} - 2I_xI_yI_{xy} + (1+I_y^2)I_{xx}}{(1+I_x^2+I_y^2)^2}. \tag{6}$$

In [30, 13], methods for constraining the evolution and the construction of convergent schemes based on the knowledge of the noise variance, were reported. Extensions of the Beltrami flow for texture images in which orientation needs to be preserved were reported in [12].

Denote the different channels by I^i, where i is an index indicating the channel number. E.g. for color images we have $I^1 = R$, $I^2 = G$ and $I^3 = B$. Let us also add the oversimplified assumption that the R, G, B color space may be considered a Euclidean space. For the Euclidean multi channel case, the norm we consider is $\int \sqrt{g}$. Here g is the determinant of the metric matrix $g = \det(g_{ij}) = g_{11}g_{22} - g_{12}^2$ given by its components $g_{\mu\nu} = \delta_{\mu\nu} + \sum_i I^i_\mu I^i_\nu$. This action functional is given explicitly by

$$S = \int \sqrt{1 + \sum_i |\nabla I^i|^2 + \frac{1}{2}\sum_{ij}(\nabla I^i, \nabla I^j)^2 dxdy}, \tag{7}$$

where $(\nabla R, \nabla G) \equiv R_xG_y - R_yG_x$ stand for the magnitude of the vector product (cross) of the vectors ∇R and ∇G. The action in Eq. (7) is simply the area of the image as a surface.

Let us explore the effects of scaling the intensity axis. If we multiply the intensities by a constant β, the above norm may be read as

$$S = \int \sqrt{1 + \beta^2 \sum_i |\nabla I^i|^2 + \beta^4 \frac{1}{2}\sum_{ij}(\nabla I^i, \nabla I^j)^2 dxdy}. \tag{8}$$

The steepest descent flow for this functional depends on the value of β. For $\beta \gg \sup_{i,\mathbf{x}}|\nabla I^i|$ it practically means mapping the intensity values that usually range between 0 and 255 to, let say, $[0, 1000]$. Roughly speaking, for this limit of β, the order of events along the scale of the flow is as follows: First the channels are aligned together, and only then starts the selective smoothing geometric flow (similar to the single channel TV-L_1). On the other limit, where $\beta \ll \sup_{i,\mathbf{x}}|\nabla I^i|$, the smoothing will tend to occur uniformly in all directions as a multi channel heat equation (L_2).

3 Coupling Requirements

When considering multi channel images we need to define the way the channels are to be coupled. The question is how should we link between the different channels. Assume that each channel is 'equally important' and thus the measure that links between the different channels should be symmetric in this aspect. Within the scale space philosophy, we want the different channels to get smoother in scale. This requirement leads to the minimization of the different channels gradient magnitudes $|\nabla I^i|$ combined in one why or another that yields coupling.

$\hat{\mathbf{N}}(\mathbf{x})$ onto the light source direction $\vec{l}$, multiplied by the albedo $\rho(x,y)$. The albedo captures the characteristics of the 3D object's material, and is different for each spectral channel. That is, the 3 color channels may be written as

$$\begin{aligned} I^R(\mathbf{x}) &= \rho_R(\mathbf{x})\hat{\mathbf{N}}(\mathbf{x})\cdot\vec{l} \\ I^G(\mathbf{x}) &= \rho_G(\mathbf{x})\hat{\mathbf{N}}(\mathbf{x})\cdot\vec{l} \\ I^B(\mathbf{x}) &= \rho_B(\mathbf{x})\hat{\mathbf{N}}(\mathbf{x})\cdot\vec{l}. \end{aligned} \tag{9}$$

This means that the different colors capture the change in material via ρ_i (where i stands for R, G, B) that multiplies the normalized shading image $\tilde{I}(\mathbf{x}) = \hat{\mathbf{N}}(\mathbf{x})\cdot\vec{l}$. The above color image formation model [8] was used for color based segmentation [11] and shading extraction from color images [10]. Let us follow this model and assume that the material, and therefore the albedo, are the same within a given object in the image, e.g. $\rho_i(\mathbf{x}) = c_i$, where c_i is a given constant. Thus, $\nabla\rho_i(\mathbf{x}) = 0$ within the interior of a given object. The intensity gradient for each channel within a given object is then given by

$$\begin{aligned} \nabla I^i(\mathbf{x}) &= \tilde{I}(\mathbf{x})\nabla\rho_i(\mathbf{x}) + \rho_i(\mathbf{x})\nabla\tilde{I}(\mathbf{x}) \\ &= \tilde{I}(\mathbf{x})\nabla c_i + c_i\nabla\tilde{I}(\mathbf{x}) \\ &= c_i\nabla\tilde{I}(\mathbf{x}). \end{aligned} \tag{10}$$

Observe that, under the above assumptions, all color channels should have the same gradient direction within a given object.

Next we deal with the boundaries between objects. Since along the boundaries, both the normalized shading image $\tilde{I}$ and the albedo ρ_i go through a sudden change. The gradient direction should be orthogonal to the boundary for each of the channels.

Following the above claims, the first step in multi channel image processing is the alignment of the channels so that their gradient directions agree. Next comes the diffusion of all the channels simultaneously, while verifying that the alignment property holds. For a large enough β, Eq. (8) follows exactly these requirements. Note also that for a large enough β, the area norm Eq. (8) is a regularization form of

$$\int\sqrt{\sum_i |\nabla I^i|^2 + \beta^2\sum_{ij}(\nabla I^i, \nabla I^j)^2}\,dxdy, \tag{11}$$

that captures the right order of events as described above. If we also add the demand that edges should be preserved and search for the simplest geometric parametrization for the flow, we end up with the Beltrami flow as a natural selection. In the next section we summarize [37] with a brief review on line element theories in color.

3.2 Line Element Theories in Color

More than a hundred years ago, physicists started to describe the human color perception as simple geometric space. At the end of the last century [33] Helmholtz was the first to define a 'line element' (arclength) in color space. He used a Euclidean R, G, B defined by the arclength

$$ds^2 = dR^2 + dG^2 + dB^2. \tag{12}$$

This model failed to represent empirical data of human color perception. Schrödinger [28, 27] fixed Helmholtz model by introducing the arclength

$$ds^2 = \frac{1}{l_R R + l_G G + l_B B}\left(\frac{l_R(dR)^2}{R} + \frac{l_G(dG)^2}{G} + \frac{l_B(dB)^2}{B}\right), \tag{13}$$

where l_R, l_G, l_B are constants. Schrödinger's model was later found to be inconsistent with findings on threshold data of color discrimination. Next, Stiles [32] introduced the arclength

$$ds^2 = \left(l_R\frac{9dR}{1+9R}\right)^2 + \left(l_G\frac{9dG}{1+9G}\right)^2 + \left(l_B\frac{9dB}{1+9B}\right)^2, \tag{14}$$

where again, l_R, l_G, l_B are constants. Note that Stiles' color space can be smoothly mapped into a Euclidean space. The mapping to Euclidean space is $\tilde{R} = l_R \ln(1+9R)$ that yields $d\tilde{R} = l_R\frac{9dR}{1+9R}$.

Half a generation later, Vos and Walraven [34] introduced the 'most elaborate' arclength according to [37]:

$$ds^2 = g_{ij}dI^i dI^j, \tag{15}$$

where I^i $i = 1, 2, 3$ stands for R, G, B, and the g_{ij} coefficients are functions of R, G, and B. Vos and Walraven have also incorporated other perception mechanisms within the definition of their arclength. Like Schrödinger's color space, Vos-Walraven's model is not Euclidean.

If we summarize the available models for color space, we have two main cases:

1. The first is the *inductive* line elements that derive the arclength by simple assumptions on the visual response mechanisms. For example, we can assume that the color space can be simplified and represented as a Riemannian space with zero Gaussian curvature, i.e. can be smoothly mapped into a Euclidean space. E.g. Helmholtz and Stiles models. Then, the arclength ('line element') in the Euclidean space is given by

$$ds_c^2 = dR^2 + dG^2 + dB^2. \tag{16}$$

   Another possibility for inductive line elements, is to consider color arclengths like Schrödinger or Vos-Walraven. These models define color spaces with non zero curvature ('effective' arclength).

2. We can consider *empirical* line elements in which the metric coefficients are determined to fit empirical data. Some of these models describe a Euclidean space like the CIELAB (CIE 1976 ($L^*a^*b^*$)) [37] that was recently used in [26]. Others, like MacAdam [15, 16], are based on an effective arclength.

The proposed theory and the resulting technology is not limited to zero curvature spaces, and can incorporate any inductive or empirical color line element. See for example [31].

In case we want to perform any meaningful processing operation on a given image, we need to define a spatial relation between the points in the image plane $\mathbf{x}$. As a first step define the image plane to be Euclidean, which is a straightforward assumption for 2D images, that is:

$$ds_{\mathbf{x}}^2 = dx^2 + dy^2. \tag{17}$$

Next step in the construction of any valuable geometric measure for color images is the combination of the spatial and color measures. The simplest combination for the construction of the hybrid spatial-color space is given by:

$$ds^2 = ds_{\mathbf{x}}^2 + \beta^2 ds_c^2. \tag{18}$$

For a large β it defines the natural regularization of the color space.

Given the above arclength for color images, we pose the following question: How should a given image be simplified? In other words: What is the measure/norm/functional that is meaningful? What kind of variational method should be applied in this case?

The next geometrical measure after arclength is area. Minimization of area is a well known and studied physical phenomena. The area minimization idea also fits the color image formation model as shown in the previous subsection.

Once the area is defined as a meaningful measure, one still needs to determine the parametrization for the steepest decent flow. The geometric flow for area minimization, that preserves edges the most is given by the Beltrami flow.

In the next section we present some experimental results of this flow in color.

3.3 Experimental Results

The Beltrami flow $\mathbf{I} = \Delta_g \mathbf{I}$ is used to selectively smooth the JPEG compression distortions of images that were extracted from the net. Figure 3 shows results for color image denoising via the Beltrami flow. Observe how the color perturbation along the edges are smoothed: The cross correlation between the channels holds the edge while selectively smoothing the non correlated data. Next, Figure 4 shows three snapshots for three examples of the Beltrami scale space in color.

In the last example, Figure 5 shows a snapshot from the Beltrami scale space in color. The left is the original picture. Observe that non natural color effects hardly occur even in this complicated situation at which every stroke of the artist's brush is a perceptual edge. See [35] for gray level orientation diffusion of van Gogh's pictures.

3.4 Previous Norms for Multi Channel Images

In this section we review the previous norms that were suggested for multi channel processing to further support the selection of the area norm. Let us start with two non-variational methods that will lead us to the variational norms: Chambolle [5], generalized the idea of smoothing a single valued function via a second directional derivative in the direction of minimal change. He suggested a flow by the second derivative in the direction of minimal change with respect to the channel with the largest gradient. Sapiro and Ringach [26], realized that this evolution may be computed via Di Zenzo multi valued function analysis

[6]. They named it 'color diffusion' and used the eigenvalues of the matrix (though not a metric!) $g_{\mu\nu} = \sum_i I^i_\mu I^i_\nu$ as a generalized edge detector to preserve edges.

These eigenvalues may be written as

$$\begin{aligned}\lambda_\pm &= \sum_i |\nabla I^i|^2 \pm \sqrt{\sum_{ij}(\nabla I^i \cdot \nabla I^j)^2 - \sum_{ij}(\nabla I^i, \nabla I^j)^2} \\ &= \sum_i |\nabla I^i|^2 \pm \sqrt{\sum_i |\nabla I^i|^4 + \sum_{ij, i\neq j}(\nabla I^i \cdot \nabla I^j)^2 - \sum_{ij}(\nabla I^i, \nabla I^j)^2}. \end{aligned} \tag{19}$$

Observe that the square root includes cross (vector products) and gradient magnitude in different signs. We have shown that this combination is not natural for non linear multi channel image processing.

In [24] Sapiro suggested to consider the variational method of the general form $\int f(\lambda_-, \lambda_+)$. As we have just argued, the terms that appear in the square root results in a 'weekly coupled definition' for the arclength in color space. This observation was made from a different perspective by Blomgren and Chan in [3]. They also claimed that from the class of all possible norms of the form $f(\lambda_+, \lambda_-)$, the $f(\lambda_+ + \lambda_-)$ is the most natural one. This brings us to Shah's multi channel model [29], that is based on the norm $\int \sqrt{\sum_{i=1} |\nabla I^i|^2}$ as part of a generalized Mumford-Shah functional. Observe that this term is exactly $\int \sqrt{\lambda_+ + \lambda_-}$ of Sapiro's model, i.e. $f(a, b) = \sqrt{a+b}$ which was latter analyzed in [3].

Blomgren and Chan [3] try to improve Sapiro's results and defined a different color TV norm:

$$\mathrm{TV}_m = \sqrt{\sum_{i=1}^{m} \left(\int |\nabla I^i|\right)^2},$$

with a constraint. In this case the coupling between the channels is only by the constraint. Actually, without the constraint the minimization yields a channel by channel curvature flow. Moreover, in order to obtain an efficient numerical scheme, Blomgren and Chan [3] regularize the TV into what can be shown to be a channel by channel flow towards a minimal surface coupled via the constraint. They also compared all norms that fall within the L_1 and L_2 Euclidean norms.

Non of the previous norms included the cross-alignment terms in a proper way.

4 Conclusion

The geometric framework of images as surfaces lead us to the norm that resolves the twist (torsion) between the channels via the cross-alignment term. It is very important for image reconstruction after distortion of the different channels. This was demonstrated by our example in which color fluctuations occur along the edges as a result of JPEG lossy compression. In order to preserve the edge and resolve these fluctuations one needs to use the cross alignment within the definition of the norm.

The geometric framework with the area ($\int \sqrt{g}$) norm, yields a natural coupling between the channels via the Beltrami flow that preserves edges in a geometrical way. The cross alignment and the gradient magnitude terms appear as proper measures in the definition of the area norm. We have shown that the geometric framework yields the most natural norm with respect to all previous existing norms, and with respect to a list of objective requirements and considerations of the color image formation, and color perception process.

5 Acknowledgments

I thank Nir Sochen, Ravi Malladi, and Freddy Bruckstein for interesting discussions on the importance of a natural geometric norm in scale space theory, and line element theories in color.

References

[1] L Alvarez, F Guichard, P L Lions, and J M Morel. Axioms and fundamental equations of image processing. *Arch. Rational Mechanics*, 123, 1993.

[2] L Alvarez, P L Lions, and J M Morel. Image selective smoothing and edge detection by nonlinear diffusion. *SIAM J. Numer. Anal*, 29:845–866, 1992.

[3] P Blomgren and T F Chan. Color TV: Total variation methods for restoration of vector valued images. cam TR, UCLA, 1996.

[4] V Caselles, R Kimmel, G Sapiro, and C Sbert. Minimal surfaces: A geometric three dimensional segmentation approach. *Numerische Mathematik*, to appear, 1996.

[5] A Chambolle. Partial differential equations and image processing. In *Proceedings IEEE ICIP*, Austin, Texas, November 1994.

[6] S Di Zenzo. A note on the gradient of a multi image. *Computer Vision, Graphics, and Image Processing*, 33:116–125, 1986.

[7] A I El-Fallah, G E Ford, V R Algazi, and R R Estes. The invariance of edges and corners under mean curvature diffusions of images. In *Processing III SPIE*, volume 2421, pages 2–14, 1994.

[8] P T Eliason, L A Soderblom, and P S Chavez. Extraction of topographic and spectral albedo information from multi spectral images. *Photogrommetric Engineering and Remote Sensing*, 48:1571–1579, 1981.

[9] L M J Florack, A H Salden, , B M ter Haar Romeny, J J Koendrink, and M A Viergever. Nonlinear scale-space. In B M ter Haar Romeny, editor, *Geometric–Driven Diffusion in Computer Vision*. Kluwer Academic Publishers, The Netherlands, 1994.

[10] B V Funt, M S Drew, and M Brockington. Recovering shading from color images. In G Sandini, editor, *Lecture Notes in Computer Science, 588, Computer Vision: ECCV'92*, pages 124–132. Springer-Verlag, 1992.

[11] G Healey. Using color for geometry-insensitive segmentation. *J. Opt. Soc. Am. A*, 6:920–937, 1989.

[12] R Kimmel, N Sochen, and R Malladi. On the geometry of texture. Report LBNL-39640, UC-405, Berkeley Labs. UC, CA 94720, November 1996.

[13] R Kimmel, N Sochen, and R Malladi. From high energy physics to low level vision. In *Lecture Notes In Computer Science: First International Conference on Scale-Space Theory in Computer Vision*. Springer-Verlag, 1997.

[14] R Kimmel, N Sochen, and R Malladi. Images as embedding maps and minimal surfaces: Movies, color, and volumetric medical images. In *Proc. of IEEE CVPR'97*, Puerto Rico, June 1997.

[15] D L MacAdam. Visual sensitivity to color differences in daylight. *J. Opt. Soc. Am.*, 32:247, 1942.

[16] D L MacAdam. Specification of small chromaticity differences. *J. Opt. Soc. Am.*, 33:18, 1943.

[17] R Malladi and J A Sethian. Image processing: Flows under min/max curvature and mean curvature. *Graphical Models and Image Processing*, 58(2):127–141, March 1996.

[18] D Mumford and J Shah. Boundary detection by minimizing functionals. In *Proceedings of CVPR, Computer Vision and Pattern Recognition*, San Francisco, 1985.

[19] P Perona and J Malik. Scale-space and edge detection using anisotropic diffusion. *IEEE-PAMI*, 12:629–639, 1990.

[20] A M Polyakov. *Physics Letters*, 103B:207, 1981.

[21] M Proesmans, E Pauwels, and L van Gool. Coupled geometry-driven diffusion equations for low level vision. In B M ter Haar Romeny, editor, *Geometric–Driven Diffusion in Computer Vision*. Kluwer Academic Publishers, The Netherlands, 1994.

[22] In B M ter Haar Romeny, editor, *Geometric–Driven Diffusion in Computer Vision*. Kluwer Academic Publishers, The Netherlands, 1994.

[23] L Rudin, S Osher, and E Fatemi. Nonlinear total variation based noise removal algorithms. *Physica D*, 60:259–268, 1992.

[24] G Sapiro. Vector-valued active contours. In *Proceedings IEEE CVPR'96*, pages 680–685, 1996.

[25] G Sapiro and D Ringach. Anisotropic diffusion of multivalued images. In *12th Int. Conf. on Analysis and Optimization of Systems: Images, Wavelets and PDE'S*, Paris, June 1996. Springer Verlag.

[26] G Sapiro and D L Ringach. Anisotropic diffusion of multivalued images with applications to color filtering. *IEEE Trans. Image Proc.*, 5:1582–1586, 1996.

[27] E Schrödinger. Grundlinien einer theorie der farbenmetrik in tagessehen. *Ann. Physik*, 63:481, 1920.

[28] E Schrödinger. Theorie der pigmente von grösster leuchtkraft. *Ann. Physik*, 62:603, 1920.

[29] J Shah. Curve evolution and segmentation functionals: Application to color images. In *Proceedings IEEE ICIP'96*, pages 461–464, 1996.

[30] N Sochen, R Kimmel, and R Malladi. From high energy physics to low level vision. Report LBNL 39243, LBNL, UC Berkeley, CA 94720, August 1996. $http://www.lbl.gov/\sim ron/belt-html.html.$

[31] N Sochen and Y Y Zeevi. Using Vos-Walraven line element for Beltrami flow in color images. EE-Technion and TAU HEP report, Technion and Tel-Aviv University, March 1997.

[32] W S Stiles. A modified Helmholtz line element in brightness-colour space. *Proc. Phys. Soc. (London)*, 58:41, 1946.

[33] H Helmholtz von. *Handbuch der Psychologishen Optik.* Voss, Hamburg, 1896.

[34] J J Vos and P L Walraven. An analytical desription of the line element in the zone-fluctuation model of colour vision II. The derivative of the line element. *Vision Research*, 12:1345–1365, 1972.

[35] J Weickert. *Anisotropic diffusion in image processing.* Ph.D. thesis, Kaiserslautern Univ., Kaiserslautern, Germany, November 1995.

[36] R Whitaker and G Gerig. Vector-valued diffusion. In B M ter Haar Romeny, editor, *Geometric–Driven Diffusion in Computer Vision.* Kluwer Academic Publishers, The Netherlands, 1994.

[37] G Wyszecki and W S Stiles. *Color Science: Concepts and Methods, Qualitative Data and Formulae, (2nd edition).* Jhon Wiley & Sons, 1982.

[38] A. Yezzi. Modified curvature motion for image smoothing and enhancement. *IEEE Trans. IP*, page This issue, 1997.

Figure 3: Denoising JEPG lossy compression perturbations. Rows 1&3: The original image and the three channels (R,G,B). Rows 2&4: The result of the Beltrami color flow (70 numerical iterations, $\Delta t = 0.21$, $\Delta x = 1$). [This is a color figure]

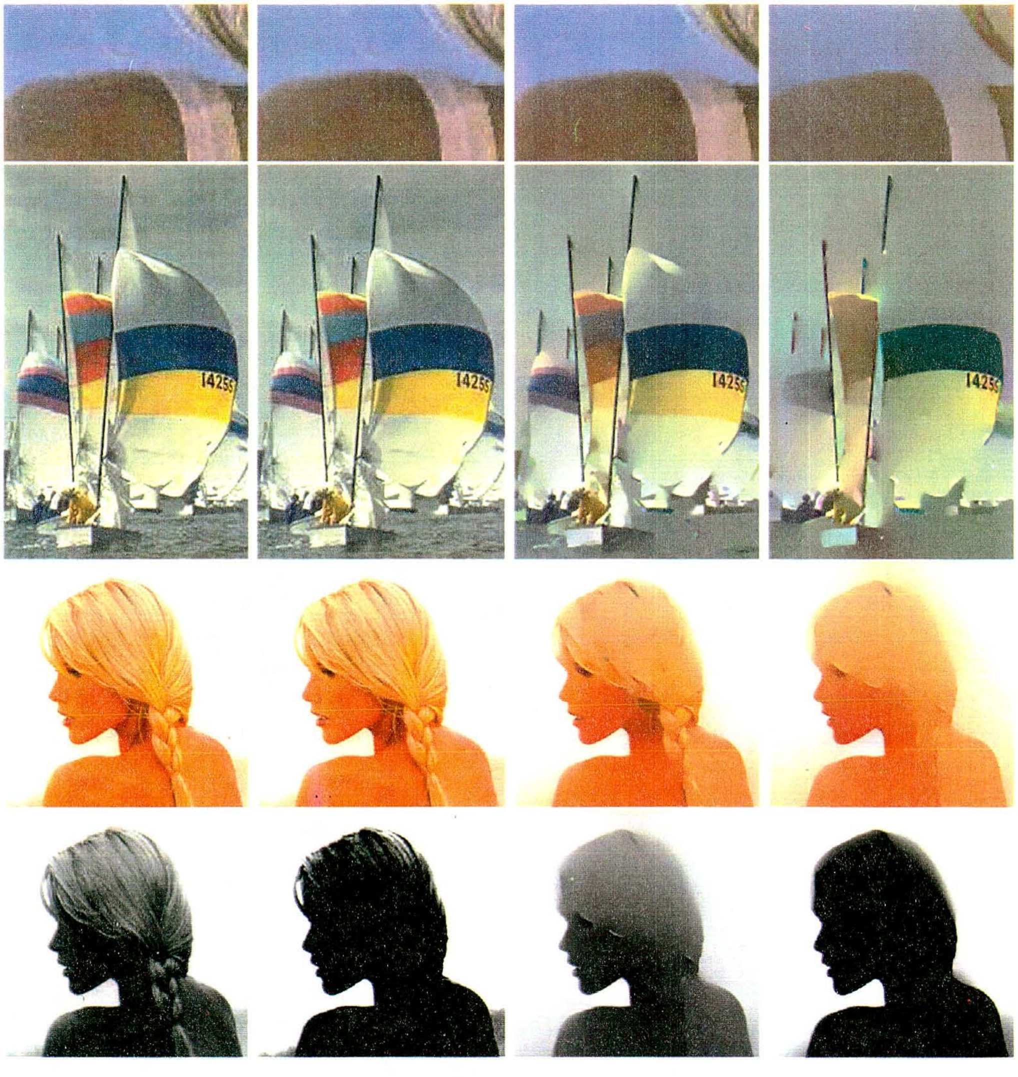

Figure 4: Rows 1,2&3: Three snapshots along the scale space for a color image of three color images (left most is the original image). Bottom row: The blue channel and a soft threshold of the original and the last image, demonstrating the edge preserving property of the flow. [This is a color figure]

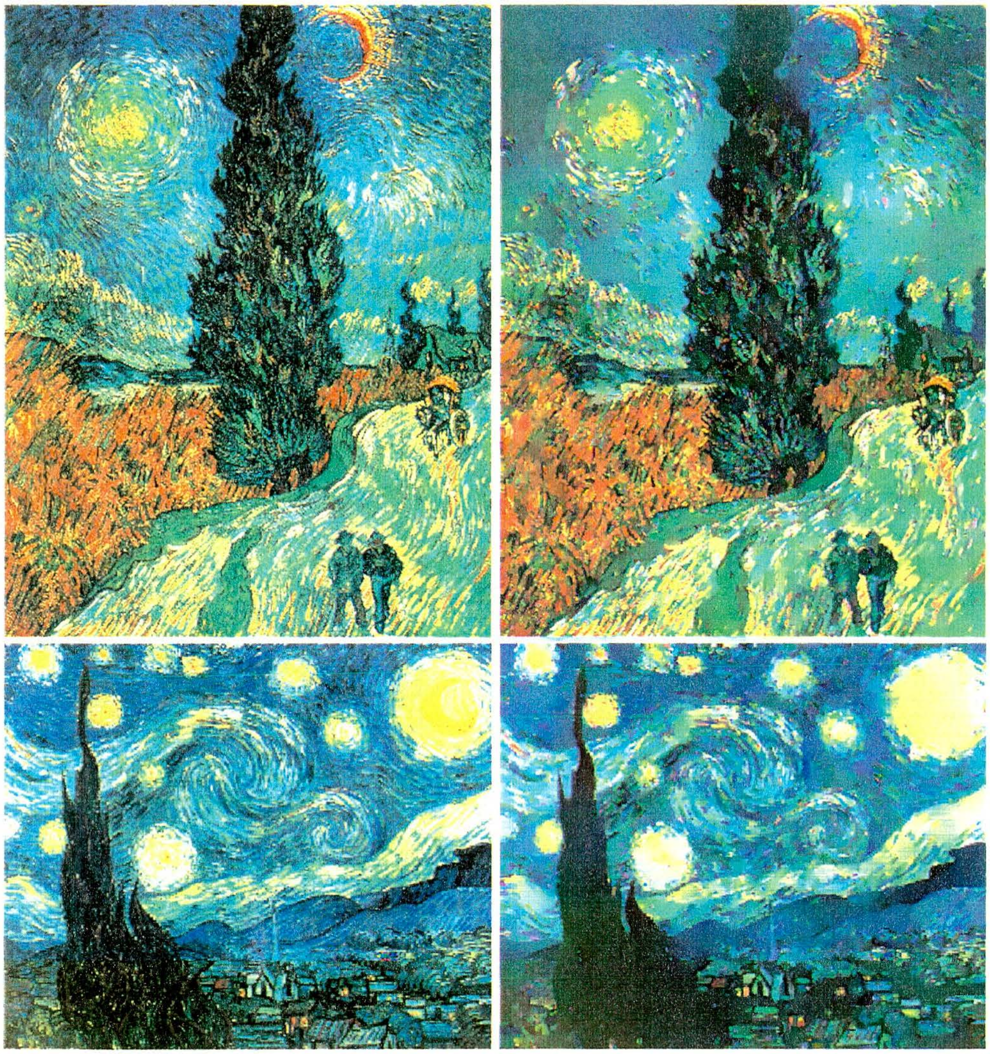

Figure 5: A snapshot from the color scale space for van Gogh's *Lane under Cypresses below the Starry Sky*, and *Starry night*. Left is the original image. [This is a color figure]

Ernest Orlando Lawrence Berkeley National Laboratory
One Cyclotron Road | Berkeley, California 94720

Prepared for the U.S. Department of Energy under Contract No. DE-AC03-76SF00098